

Manipulation of plasma grating by impulsive molecular alignment

Peifen Lu, Jian Wu, and Heping Zeng^{a)}

State Key Laboratory of Precision Spectroscopy, East China Normal University, Shanghai 200062, China

(Received 13 October 2013; accepted 15 November 2013; published online 27 November 2013)

We experimentally demonstrated that multiphoton-ionization-induced plasma grating in air could be precisely manipulated by impulsive molecular alignment. In the linear region, the impulsively aligned molecules modulated the diffraction efficiency of the plasma grating for a time-delayed femtosecond laser pulse. In the nonlinear region, the third harmonic generation from the plasma grating was either enhanced or suppressed by following the alignment of the molecules. © 2013 AIP Publishing LLC. [<http://dx.doi.org/10.1063/1.4837035>]

Filamentation of self-guided propagation of intense ultrashort laser pulses in gases, e.g., atmosphere air, has been extensively studied for its interesting applications for light-guiding,¹ pulse compression,² nonlinear frequency conversion,³ supercontinuum generation,⁴ remote sensing,⁵ and THz generation.⁶ In molecular gas by steering the spatial alignment of molecules, the filamentation and the consequent nonlinear effects can be manipulated, such as the length of the self-guided filaments,^{7,8} supercontinuum generation,^{9–11} and spectral modulation^{12–14} of ultrashort laser pulses, THz radiation,¹⁵ and interaction of two closely propagating filaments.^{16–18} The photonic plasma grating can be generated by non-collinear interaction of two crossing filaments,^{19,20} which featured with a spatial period of several micrometers and high damage threshold as photonic devices for high-intensity laser applications. It was demonstrated that the plasma grating could transport the photon energy from one beam to another²¹ as a linear diffraction device and dramatically enhance the third harmonic generation (THG)²⁰ as a nonlinear media.

In this Letter, we demonstrate that the plasma grating created by the interaction of two non-collinear filaments in air can be manipulated by steering the spatial alignment of the contained N₂ and O₂ molecules. Our results show that both the linear diffraction efficiency of a time-delayed femtosecond laser pulse and the nonlinear THG from the plasma grating can be controlled by the quantum revivals of the impulsively aligned molecules. Beyond the control of single filament, we demonstrate that the molecular alignment can be applied to manipulate the plasma grating in air as a photonic device for high-intensity laser applications.

The experimental setup is schematically shown in Fig. 1(a). A femtosecond laser pulse (50 fs, 800 nm, 1 kHz) from a Ti:Sapphire amplifier laser system was equally split into two parts in energy. Each part passed a second-order nonlinear Beta-Barium Borate crystal (β -BBO) to produce the second harmonic (SH) pulse. The SH pulse was separated from the fundamental-wave (FW) one with a dichroic mirror (HR@800/AR@400 nm). Finally four arms were obtained, which consisted of two FW and two SH pulses, respectively, labeled as FW1, FW2, SH1, and SH2. The polarization of SH1 could be changed by a half-wave plate at 400 nm. In our

experiments, the FW1, FW2, and SH1 pulses were horizontally polarized, while the SH2 pulse was vertically polarized. The time delay delay1 was adjusted to synchronize the FW1 and FW2 pulses for plasma grating generation through multi-photon ionizing the molecules in air. The time delays of the SH1 and SH2 with respect to the formation of the plasma grating, labeled as delay2 and delay3, were adjusted with two motorized stages. By using two lens of $f=50$ cm, both FW1 and FW2 pulses were focused to produce two non-collinear filaments in air with a small crossing angle θ_G to create a plasma grating. The length of each individual filament was measured to be ~ 2 cm. The SH1 was focused by a lens of $f=60$ cm and then combined collinearly with FW1 with a dichroic mirror (HR@800/AR@400 nm), acting as a pump pulse to impulsively align the molecules in the region where the plasma grating was formed. The energies of FW1 and FW2 pulses were set to be equal (~ 1.35 mJ) for a maximum modulation depth of the plasma grating. The energy of SH1 pulse for the impulsive molecular alignment was ~ 0.24 mJ.

To measure the diffraction efficiency of the created plasma grating, the attenuated SH2 pulse was weakly focused by a lens of $f=80$ cm onto the plasma grating with a crossing angle φ with respect to the propagation direction of FW2. For the fairly low intensity of SH2 pulse, no nonlinear effect was expected for SH2 itself. The diffracted pulse of the incident SH2 pulse by the plasma grating was tightly focused by a lens of $f=10$ cm onto a photodetector. To study the modulation of the nonlinearity of the formed plasma grating, the third harmonic (TH) pulse generated from FW2 pulse was separated from the collinear FW2 pulse by using a prism, whose intensity was measured by a photomultiplier tube (PMT). A lock-in amplifier was used to achieve a good signal-to-noise ratio. In order to directly image the plasma grating induced by the non-collinearly interacting filaments, the photon-ionization-induced fluorescence of the plasma grating was collected by a microscope objective (10 \times) and detected by a monochrome digital charge coupled device (CCD). The typical fluorescence image of the formed plasma grating is shown in Fig. 1(b).

When two non-collinearly crossed filaments were temporally overlapped in air, the field intensity in the interacting region followed the sinusoidal distribution due to the interference between two incident laser pulses, resulting in a

^{a)}Electronic address: hpzeng@phy.ecnu.edu.cn

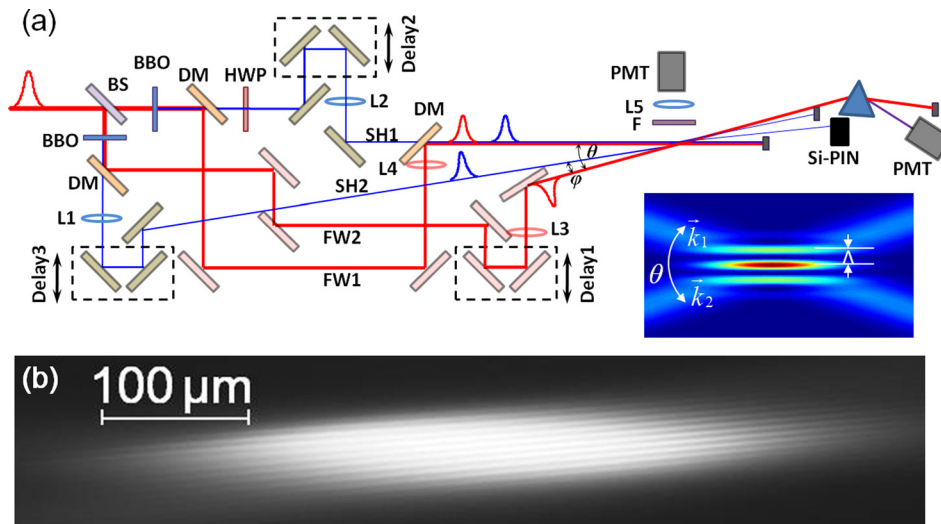


FIG. 1. (a) The schematic of the experimental setup and the formed grating structure (inset). (b) Fluorescence image of the plasma grating induced by FW1 and FW2 pulses at a crossing angle of $\theta = 10^\circ$.

volume of plasma with periodic microstructures due to the multi-photon ionization of the molecules, i.e., plasma grating which persisted for tens of picoseconds. The grating period $\Lambda = \lambda_{FW}/[2 \sin(\theta_G/2)]$ varied with the crossing angle θ_G , where λ_{FW} is the central wavelength of the FW pulses used to form the plasma grating. In our experiment, the value of Λ was expected to be $4.59 \mu\text{m}$ at $\theta_G = 10^\circ$, which agreed well with $\Lambda \sim 4.71 \mu\text{m}$ measured from the captured fluorescence image of the plasma grating as shown in Fig. 1(b). The effective thickness D of the plasma grating was estimated to be $100 \mu\text{m}$, so $\gamma = D/\Lambda \sim 21$ (larger than 10), indicating that it was a volume plasma grating. For the volume grating, the diffraction of the time-delay SH2 pulse was governed by Bragg equation of $2\Lambda \sin \theta_B = n\lambda_{SH}$ ($n = 0, \pm 1, \pm 2, \dots$), where λ_{SH} is the wavelength of the diffracted SH pulse and θ_B is the scattering angle. In our experiment for $\varphi = \theta_G/4$, the scattering angle $\theta_B = \theta_G/2 - \theta_G/4 = \theta_G/4$. For small crossing angle θ_G and $n = 1$, the SH2 probe pulse satisfied the Bragg condition for the first-order scattering. To study the diffraction by the plasma grating and meanwhile avoid the Kerr and other effects around the zero time delay, the probe pulse of SH2 was temporally delayed by 1.5 ps with respect to the synchronized FW1 and FW2 pulses.

For a time-delayed probe pulse at a Bragg incident angle, the diffraction efficiency was determined by the modulation depth of the refractive index of the plasma grating, i.e., the photon-ionization-induced electron density. The strong field ionization rate for neutral molecules steeply depends on its relative orientation with respect to the polarization of the laser field. We therefore could control the plasma density of the created photonic grating by steering the alignment of the molecules with respect to polarization of the incident FW1 and FW2 pulses.

We used the advanced SH1 pulse to impulsively align the N_2 and O_2 molecules in air before the formation of the plasma grating. Due to the rephasing of the rotational wavepacket of the molecules impulsively excited by the SH1 pulse, the molecules could periodically orientate parallel or perpendicular to the polarization of the FW1 and FW2 pulses after the end of the SH1 pulse. Owing to electron-localization-assisted enhanced ionization of the diatomic molecules along the polarization of the laser field,²² the N_2 and O_2

molecules aligned parallel to the field polarization showed much higher ionization probabilities than the perpendicular molecules.²³ Consequently, when the intense FW1 and FW2 pulses arrived and experienced the pre-aligned molecules, the photon ionization probabilities of the N_2 and O_2 molecules were either enhanced for parallel aligned molecules or suppressed for perpendicular ones. Considering the sinusoidal field intensity distribution of the crossed FW pulses and molecular-orientation-dependent ionization probability, the macroscopic refractive index modulation could be controlled by molecular alignment.

To verify the modulation of the plasma grating induced by molecular alignment, we fixed the time delay of the SH2 probe pulse, i.e., delay3, and tuned the time delay between the SH1 pump pulse and grating forming pulses, i.e., delay2. As shown in Fig. 2(a), a modulation of the diffraction efficiency of the SH2 pulse by the periodical revivals of the molecular alignment was clearly visible with a maximum modulation depth of $\sim 14\%$. Around the half revival of the impulsively aligned N_2 , the energy of the diffracted SH2 pulse first increased (delay A) and then decreased (delay B) due to the enhanced and decreased modulation depth of the plasma grating, which were attributed to the orientation-dependent ionization of the molecules for the formation of the plasma grating by the non-collinearly crossed FW pulses. We also investigated the fluorescence intensity of the molecular ions inside the plasma grating. A modulation of the fluorescence intensity of the plasma grating was observed by following the alignment of the N_2 and O_2 molecules in air, as plotted in Fig. 2(b). The fluorescence intensity of the plasma grating was increased and decreased when it was formed in the presence of parallel and perpendicularly pre-aligned molecules, respectively.

To investigate the role of the impulsive molecular alignment on the optical nonlinearity of the plasma grating, we measured the THG from the plasma grating as a function of molecular alignment. The experimental results clearly showed the dependence of the THG process on the molecular alignment, as presented in Fig. 3 (red line). The energy of the generated TH pulse increased and decreased, respectively, when the molecules aligned parallel (delay A) or perpendicular (delay B) to the polarization of the incident FW1

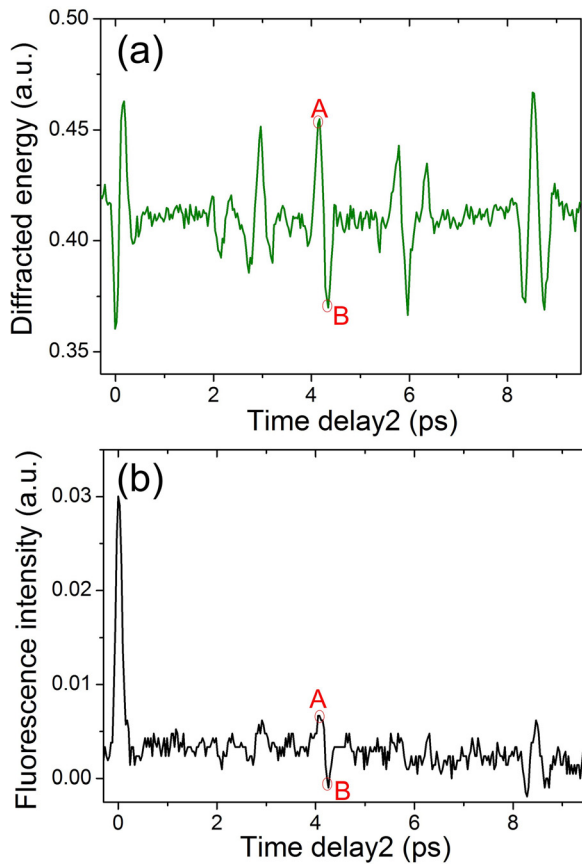


FIG. 2. (a) Modulation of the diffracted SH energy and (b) fluorescence signal of N_2^+ (or O_2^+) in the plasma grating versus the time delay delay2.

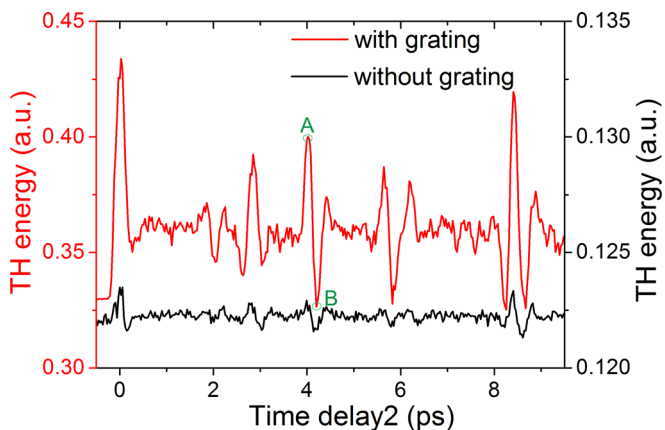


FIG. 3. Modulation of the THG from FW2 pulse by the impulsively aligned molecules with (red) and without (black) the plasma grating. The energy of SH1 pulse was set to be ~ 0.24 mJ.

and FW2 pulses. To make sure that the control of the THG came from the modulation of the formed plasma grating but not a single filament, we blocked the FW1 pulse and measured the energy of the generated TH pulse from FW2 by tuning delay2. As shown in Fig. 3 (black line), the molecular-alignment-induced modulation of the THG from a single filament dramatically shrank, indicating the significant role of the plasma grating for the THG. The pre-aligned molecules not only modulated the third-order susceptibility $\chi^{(3)}$ as demonstrated in Ref. 24 to control the THG from a single pulse,

but also more importantly as demonstrated here the formation of the plasma grating and its optical nonlinearity, e.g., the THG.

In summary, we have experimentally demonstrated that the plasma grating induced by two non-collinearly crossed femtosecond filaments could be precisely manipulated by the impulsive molecular alignment. The linear grating diffraction efficiency could be improved and THG from the plasma grating could be enhanced when the plasma grating was created in the presence of the parallel aligned molecules. The molecular alignment therefore provides a practical method to control the features of the photon-ionization-induced plasma grating in molecular gas, such as atmosphere air, as a photonic device for high-intensity laser applications.

We acknowledge financial supports from the National Basic Research Program of China (2011CB808105), National Natural Science Fund of China (11274115 and 10990101), International Science and Technology Collaboration Program (2010DFA04410 and 11530700900), Chinese Education Ministry Reward for Excellent Doctors in Academics (MXRZZ2010008), and National Key Scientific Instrument Project (2012YQ150092).

¹M. Rodriguez, R. Sauerbrey, H. Wille, L. Woëste, T. Fujii, Y.-B. André, A. Mysyrowicz, L. Klingbeil, K. Rethmeier, W. Kalkner, J. Kasparian, E. Salmon, J. Yu, and J.-P. Wolf, *Opt. Lett.* **27**, 772 (2002).

²A. Couairon, M. Franco, A. Mysyrowicz, J. Biegert, and U. Keller, *Opt. Lett.* **30**, 2657 (2005).

³S. Chin, F. Théberge, and W. Liu, *Appl. Phys. B* **86**, 477 (2007).

⁴J. Kasparian, R. Sauerbrey, D. Mondelain, S. Niedermeier, J. Yu, J. P. Wolf, Y. André, M. Franco, B. Prade, S. Tzortzakis, A. Mysyrowicz, M. Rodriguez, H. Wille, and L. Woëste, *Opt. Lett.* **25**, 1397 (2000).

⁵J. Kasparian, M. Rodriguez, G. Méjean, J. Yu, E. Salmon, H. Wille, R. Bourayou, S. Frey, Y.-B. André, A. Mysyrowicz, R. Sauerbrey, J.-P. Wolf, and L. Woëste, *Science* **301**, 61 (2003).

⁶C. D'Amico, A. Houard, S. Akturk, Y. Liu, J. Bloas, M. Franco, B. Prade, A. Couairon, V. T. Tikhonchuk, and A. Mysyrowicz, *New J. Phys.* **10**, 013015 (2008).

⁷J. Wu, H. Cai, H. Zeng, and A. Couairon, *Opt. Lett.* **33**, 2593 (2008).

⁸H. Cai, J. Wu, H. Li, X. Bai, and H. Zeng, *Opt. Express* **17**, 21060 (2009).

⁹J. Wu, H. Cai, Y. Peng, and H. Zeng, *Phys. Rev. A* **79**, 041404(R) (2009).

¹⁰H. Cai, J. Wu, Y. Peng, and H. Zeng, *Opt. Express* **17**, 5822 (2009).

¹¹H. Cai, J. Wu, X. Bai, H. Pan, and H. Zeng, *Opt. Lett.* **35**, 49 (2010).

¹²F. Calegari, C. Vozzi, S. Gasilov, E. Benedetti, G. Sansone, M. Nisoli, S. De Silvestri, and S. Stagira, *Phys. Rev. Lett.* **100**, 123006 (2008).

¹³H. Cai, J. Wu, A. Couairon, and H. Zeng, *Opt. Lett.* **34**, 827 (2009).

¹⁴J. Wu, H. Cai, A. Couairon, and H. Zeng, *Phys. Rev. A* **79**, 063812 (2009).

¹⁵J. Wu, Y. Tong, M. Li, H. Pan, and H. Zeng, *Phys. Rev. A* **82**, 053416 (2010).

¹⁶J. Wu, H. Cai, P. Lu, X. Bai, L. Ding, and H. Zeng, *Appl. Phys. Lett.* **95**, 221502 (2009).

¹⁷H. Cai, J. Wu, P. Lu, X. Bai, L. Ding, and H. Zeng, *Phys. Rev. A* **80**, 051802(R) (2009).

¹⁸J. Wu, Y. Tong, X. Yang, H. Cai, P. Lu, H. Pan, and H. Zeng, *Opt. Lett.* **34**, 3211 (2009).

¹⁹S. Suntsov, D. Abdollahpour, D. G. Papazoglou, and S. Tzortzakis, *Appl. Phys. Lett.* **94**, 251104 (2009).

²⁰X. Yang, J. Wu, Y. Peng, Y. Tong, S. Yuai, L. Ding, Z. Xu, and H. Zeng, *Appl. Phys. Lett.* **95**, 111103 (2009).

²¹X. Yang, J. Wu, Y. Tong, L. Ding, Z. Xu, and H. Zeng, *Appl. Phys. Lett.* **97**, 071108 (2010).

²²J. Wu, M. Meckel, L. Ph. H. Schmidt, M. Kunitski, S. Voss, H. Sann, H. Kim, T. Jahnke, A. Czasch, and R. Dörner, *Nat. Commun.* **3**, 1113 (2012).

²³T. Kanai, S. Minemoto, and H. Sakai, *Nature* **435**, 470 (2005).

²⁴K. Hartinger and R. A. Bartels, *Opt. Lett.* **33**, 1162 (2008).